Structural polymorphism of pyrazinium hydrogen sulfate: extending chemistry of the pyrazinium salts with small anions

Armand Budzianowski,[a]* Mariana Derzsi,[a] Piotr J. Leszczyński,[a] Michał K. Cyrański[b] and Wojciech Grochala[a,b]*

[a] ICM, The University of Warsaw, Pawińskiego 5a, 02-106, Warsaw, Poland, and [b]Faculty of Chemistry, The University of Warsaw, Pasteur 1 02-093, Warsaw, Poland

Correspondence e-mail: armand@icm.edu.pl, wg22@cornell.edu

Two polymorphs (α, β) of pyrazinium hydrogen sulfate (pyzH$^+$HSO$_4^-$, abbreviated as PHS) with distinctly different hydrogen-bond types and topologies but close electronic energies have been synthesized and characterized for the first time. The α-polymorph ($P2_12_12_1$) forms distinct blocks in which the pyzH$^+$ and HSO$_4^-$ ions are interconnected through a network of NH$\cdots$O and OH$\cdots$O hydrogen bonds. The β-form ($P\bar{1}$) consists of infinite chains of alternating pyzH$^+$ and HSO$_4^-$ ions connected by NH$\cdots$O and OH$\cdots$N hydrogen bonds. Density functional theory (DFT) calculations indicate the possible existence of a hypothetical polar $P1$ form of the β-polymorph with an unusually high dipole moment.

1. Introduction

The chemistry of pyrazinium salts is very rich and diverse. It extends from simple salts to large complexes. The simplest among them are formed by a pyrazinium cation (C$_4$N$_2$H$_5^+$, abbreviated to pyzH$^+$) and a small anion. Interestingly, up to now only four such ionic compounds have been structurally characterized: pyzH$^+$ClO$_4^-$, pyzH$^+$NO$_3^-$, pyzH$^+$BF$_4^-$ and pyzH$^+$CrClO$_3^-$ (Głowiak *et al.*, 1975; Pressprich *et al.*, 1990; Ilyukhin *et al.*, 2000; Katrusiak & Szafrański, 2006). The feature common to all of them is that they all create hydrogen bonds in order to stabilize their crystal structures. In pyzH$^+$ClO$_4^-$ (*Pbcm*), pyzH$^+$BF$_4^-$ (*Pbcm*, *C2/c*) and pyzH$^+$CrClO$_3^-$ (*Pma*2), linear NH$\cdots$N hydrogen bonds are formed between the pyrazinium cations, connecting them into infinite one-dimensional chains. The anions do not participate in hydrogen bonding but are held in between the chains by van der Waals interactions (Fig. 1*a*). The crystal structures of these salts can be described as composed of alternating cationic and anionic layers. The case of pyzH$^+$NO$_3^-$ (*P2$_1$/c*) is different. Here, the pyrazinium cations are completely isolated from each other by the nitrate anions. The anions play the role of hydrogen acceptors in N$\cdots$O hydrogen bonds, while forming together with the pyrazinium cations isolated hydrogen-bonded pyzH$^+\cdots$ONO$_2^-$ units (Fig. 1*b*).

(I)
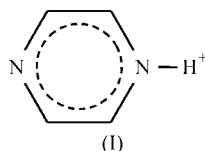
The crystal structures of pyrazinium compounds with larger anions have also been determined and the presence of hydrogen bonds is typical for the majority of them. For example, in dipyrazinium trichromate the pyrazinium cations are linked to the trichromate anion Cr$_3$O$_{10}^-$ *via* N$\cdots$O

doi:10.1107/S0108768110019580

hydrogen bonds (Pressprich *et al.*, 1988). Bifurcated NH···[O,O'] hydrogen bonds are observed for dipyrazinium tris(fluoro-trioxo-chromate) (Sendil & Ozgun, 2006). Only one pyrazinium compound, a high-temperature form of pyzH$^+$BF$_4^-$ ($P2_1/n$), does not contain NH···N hydrogen bonds. There are only very weak heteronuclear NH···F bonds that link pyzH$^+$ and BF$_4^-$ (Katrusiak & Szafrański, 2006).

In this work we report the synthesis and structural characterization of two polymorphic forms (α and β) of a novel simple pyrazinium salt, pyrazinium hydrogen sulfate (pyzH$^+$HSO$_4^-$, abbreviated as PHS). Both polymorphs show distinct hydrogen-bond topologies (Figs. 1c and d) which are very different from those present in the previously reported pyrazinium salts (Figs. 1a and b). Additionally, we use the
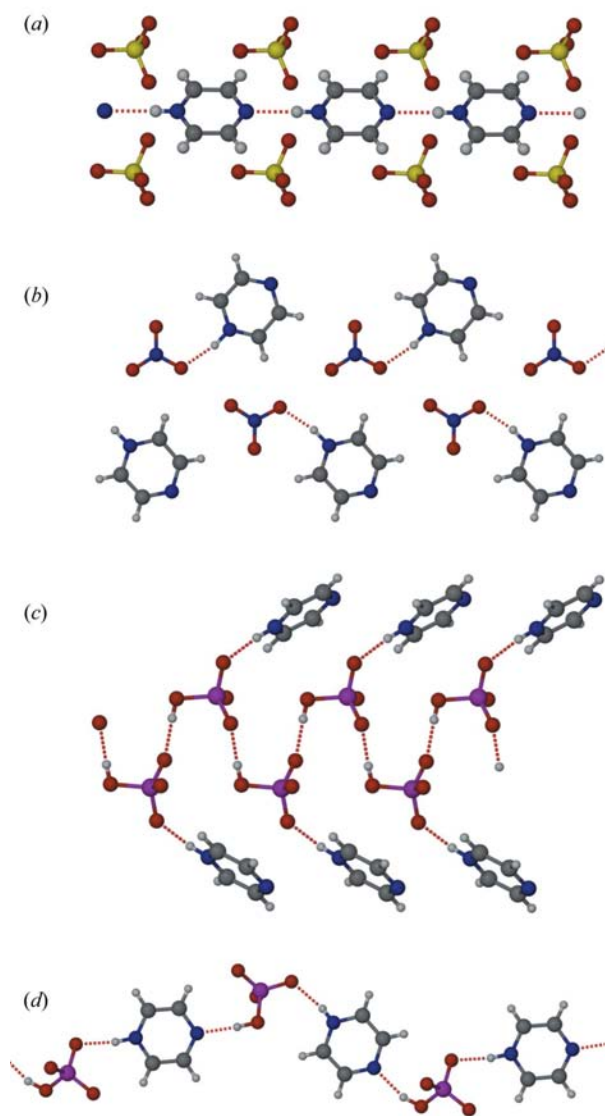
Figure 1
Hydrogen-bond topologies present in simple pyrazinium salts: (a) NH···N one-dimensional networks in pyzH$^+$ClO$_4^-$ (Głowiak *et al.*, 1975; Ilyukhin *et al.*, 2000; Katrusiak & Szafrański, 2006); (b) isolated NH···O hydrogen bonds in pyzH$^+$NO$_3^-$ (Katrusiak & Szafrański, 2006); (c) NH···O and OH···O hydrogen bonds in α-pyzH$^+$HSO$_4^-$ (this work); (d) NH···O and OH···N hydrogen bonds in β-pyzH$^+$HSO$_4^-$ (this work).

theoretical DFT approach to calculate the total energies of the two polymorphs and show that the β-form could exist in two distinct states; the experimental form and also in a hypothetical polar form with an unusually large dipole moment. Our calculations suggest that a small energetic barrier exists between the two states of the β-form of different polarities, suggesting that the polarization of the experimental $P\bar{1}$ form by an external electric field should be feasible.

2. Methodology

2.1. Synthesis

α-PHS has been synthesized from sulfuric acid and pyrazine in a 1:1 ratio in water. Excess water was removed *in vacuo* until an oily residue was obtained. The crude crystalline product was collected by adding thf. Crystallization was performed from a Et$_2$O/MeOH mixture (volume ratio of 1:1).

Very small amounts of β-PHS (insufficient for characterization other than structural) have been obtained as a byproduct of a prolonged (3 months) chemical decomposition of di(pyrazine)silver(II) peroxydisulphate in moist air (Leszczyński *et al.*, 2010). Crystals of β-PHS were manually separated from other products of chemical decomposition using an optical microscope. All operations for dry hygroscopic samples were performed inside an Ar-filled glovebox (MBraun). Both polymorphs were found to be stable for prolonged periods of time at temperatures between 103 and 293 K, when kept in argon gas.

2.2. Single-crystal X-ray measurements

Crystals of the α-PHS polymorph show electrostatic attraction to the microtool, reflect a broad range of colours under polarized light and are very unstable in atmosphere (see Fig. S1 in the supplementary material,[1] SM2). In our X-ray measurements high-quality colourless crystals were used: a 1.0 × 0.2 × 0.2 mm needle of α-PHS and a 0.2 × 0.1 × 0.1 mm prism of β-PHS. Crystals were protected from the atmosphere using silicon oil at low temperatures and a colourless lacquer at room temperature. The measurements were carried out using the four-circle kappa Oxford diffractometer KM4-CCD equipped with an Oxford Cryosystem device. The distance between the crystal and the CCD camera was 62 mm.

Data reduction and analysis were carried out with the Oxford Diffraction programs (Oxford Diffraction, 2002). Structures were solved and refined using the programs *SHELXS*97 and *SHELXL*97 (Sheldrick, 2008). Lorentz–polarization and absorption corrections were applied. Structures were refined by full-matrix least squares with anisotropic temperature factors for heavy atoms. All H atoms have been successfully located from the Fourier map; geometry constraints have only been applied for all the H atoms in the aromatic ring in the β-polymorph except those forming hydrogen bonds. The crystal and structural data for both

---

Table 1
Crystal data and experimental details for α-PHS (at 103 and 293 K) and β-PHS (at 100 K).

For all structures: $C_4H_5N_2 \cdot HO_4S$, $M_r = 178.17$, $Z = 4$. Experiments were carried out with Mo $K\alpha$ radiation. Refinement was with 0 restraints. H atoms were treated by a mixture of independent and constrained refinement.

	α-PHS (103 K)	α-PHS (293 K)	β-PHS (100 K)
Crystal data			
Crystal system, space group	Orthorhombic, $P2_12_12_1$	Orthorhombic, $P2_12_12_1$	Triclinic, $P\bar{1}$
a, b, c (Å)	5.1744 (6), 9.3697 (13), 13.919 (3)	5.1748 (5), 9.4290 (11), 13.9135 (15)	5.355 (1), 7.483 (1), 16.506 (2)
α, β, γ (°)	90, 90, 90	90, 90, 90	86.484 (12), 88.111 (11), 77.487 (12)
V (Å^3)	674.83 (19)	678.88 (13)	644.38 (15)
μ (mm^{-1})	0.45	0.44	0.47
Crystal size (mm)	$1.00 \times 0.20 \times 0.20$	$1.00 \times 0.20 \times 0.20$	$0.20 \times 0.10 \times 0.10$
Data collection			
Diffractometer	KUMA KM-4CCD	KUMA KM-4CCD	KUMA KM-4CCD
Absorption correction	Multi-scan	Multi-scan	Multi-scan
T_{min}, T_{max}	0.665, 0.916	0.666, 0.917	0.910, 0.954
No. of measured, independent and observed [$I > 2\sigma(I)$] reflections	6079, 1555, 1488	6199, 1593, 1459	12 016, 3124, 1242
R_{int}	0.022	0.025	0.109
Refinement			
$R[F^2 > 2\sigma(F^2)]$, $wR(F^2)$, S	0.021, 0.058, 1.05	0.027, 0.065, 1.03	0.049, 0.109, 0.82
No. of reflections	1555	1593	3124
No. of parameters	119	118	211
$\Delta\rho_{max}, \Delta\rho_{min}$ (e Å^{-3})	0.24, −0.35	0.18, −0.36	0.37, −0.45

Computer programs used: *CrysAlis* (Oxford Diffraction, 2002), *SHELXS*97, *SHELXL*97 (Sheldrick, 2008), *X-SEED* (Barbour, 2001), *POV-Ray* (Persistence of Vision, 2004).

polymorphs are summarized in Table 1. Full structural information been deposited.

2.3. Powder X-ray measurements

The structure of α-PHS was examined as a function of temperature between 103 and 325 K. Powder X-ray diffraction (XRD) experiments for α-PHS sealed inside quartz capillaries (diameter size of 0.3 mm) have been performed using a D8 Discover diffractometer equipped with a VANTEC detector and a nitrogen Cryostream System for sample cooling. The powder XRD structure refinements show that the α-PHS does not undergo any phase transition within this temperature range (for thermal expansion of α-PHS see Fig. 2 and Fig. S2). Similar measurements were not possible for β-PHS because of an insufficient amount of high-purity material.

2.4. Melting-point determination

Determination of the melting point (409–411 K) and heat of melting (0.13 kJ mol^{-1}) of α-PHS (*cf.* Fig. S3) was carried out with a Q200 DSC analyzer (thermal analysis) and additionally confirmed by visual observations of the sample heated inside the glove-box in an inert gas atmosphere. Additionally it was confirmed outside the glove-box using Boethius apparatus VEB Wagetechnik Rapido Germany.

2.5. IR absorption spectroscopy

The middle- and far-IR spectra were measured with the Vertex 80v vacuum spectrometer (Bruker) for a fine powder of α-PHS squeezed between two AgCl or polyethylene windows, respectively. The IR spectrum of the α-polymorph collected in the wavenumber range 3800–50 cm^{-1} shows the

presence of absorption bands assigned to the pyrazinium cation and the hydrogen sulfate ion (for full assignment see Fig. S4 and Table S1 in SM). Regretfully, IR measurements were not possible for the β-polymorph due to an insufficient amount of the high-purity material.

2.6. DFT calculations

Total energy DFT calculations, including full optimization of atomic and lattice parameters, were performed using the general gradient approximation (GGA) and the projector augmented wave (PAW) method (Blöchl, 1994) with the Perdew, Burke and Ernzerhof (PBE) functionals (Perdew *et al.*, 1996) and ultrasoft Vandebildt pseudopotentials as
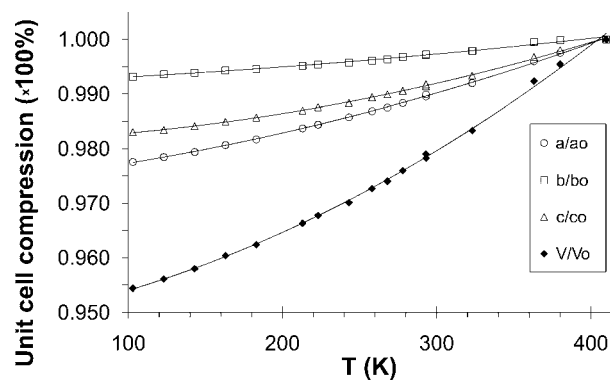
Figure 2
Thermal expansion of the unit-cell parameters of the X-ray powder diffraction data (Fig. S4) for α-PHS. All values were normalized at 410 K. The error bars for every point are smaller than the size of the graphical symbols used, thus they have been omitted for clarity.

Table 2
Geometry of hydrogen bonds in α- and β-PHS.

Experimental values measured at 103 and 100 K for α and β, respectively. All calculated values are at 0 K. For numbering of atoms see Figs. 3 and 4 (*cf.* Table S3).

Hydrogen bond		$D \cdots A$	$D{-}H$	$H \cdots A$	$D{-}H \cdots A$
α ($P2_12_12_1$)					
O4—H$\cdots$O1^{i}	Exp.	2.609 (2)	0.81 (2)	1.80 (2)	170 (2)
	Theor.	2.584	1.029	1.560	173
N3—H$\cdots$O2	Exp	2.721 (2)	0.91 (2)	1.81 (2)	173 (2)
	Theor.	2.674	1.067	1.612	172
β ($P\bar{1}$)					
N14—H$\cdots$O24	Exp	2.667 (5)	0.92 (4)	1.76 (4)	170 (4)
	Theor.	2.624	1.090	1.535	177
N24—H$\cdots$O14	Exp	2.680 (4)	0.81 (4)	1.88 (4)	169 (4)
	Theor.	2.632	1.079	1.561	171
O11—H$\cdots$N11	Exp	2.735 (5)	0.96 (4)	1.79 (4)	168 (4)
	Theor.	2.703	1.030	1.674	178
O21—H$\cdots$N21^{ii}	Exp	2.736 (4)	0.88 (4)	1.88 (4)	160 (4)
	Theor.	2.710	1.027	1.686	176

Symmetry codes: (i) $\frac{1}{2} + x, \frac{1}{2} - y + 1, -z + 2$; (ii) $x, y, z - 1$.

implemented in the Vienna *ab initio* Simulation Package, *VASP* (Kresse & Furthmüller, 1996a,b; Kresse & Joubert, 1999). The wavefunctions were expanded in plane waves of kinetic energies up to the cutoff of 500 eV. The *k*-point sampling was generated *via* the Monkhorst–Pack scheme with uniform spacing of *ca* 0.05 Å^{-1}. The electronic and ionic optimizations were carried out until the energy differences between the successive electronic and ionic cycles were less than 10^{-7} and 10^{-5} eV, respectively. Partial atomic charges (from which the dipole moment was derived) were then calculated for the optimized phases using the program *CASTEP* (Clark *et al.*, 2005) with the same settings as described above for the optimization process. All calculations were carried out formally for $p = 0$ Pa and $T = 0$ K, using unit cells ($Z = 4$) which contained 68 atoms each.

3. Results

### 3.1. α-polymorph with moderately strong NH$\cdots$O and OH$\cdots$O hydrogen bonds

PHS may formally be treated as a 1:1 adduct of pyrazine and H_2SO_4, where only half of the N atoms of pyrazine are protonated (Fig. 1c). α-PHS crystallizes in the orthorhombic $P2_12_12_1$ space group with four pyrazine cations and four hydrogen sulfate anions per unit cell; the independent part of the cell contains one cation and one anion (Fig. 3). The cations and anions are aligned into separate double chains extending along the [x] direction and lying parallel to each other in the [y] direction. The unit cell contains two such chains related to each other by twofold screw axes placed along all three crystallographic directions.

The two types of hydrogen bonds found (OH$\cdots$O and NH$\cdots$O) are both close to linear. The O$\cdots$O bond is shorter by ~ 0.1 Å than the N$\cdots$O one (Table 2). The OH$\cdots$O bonds interconnect two neighbouring hydrogen sulfate anions into a

[–HOSO–HOSO–]$_n$ chain with the $C_2^2(8)$ graph set (Etter *et al.*, 1990; Etter, 1990; Grell *et al.*, 1999). Each anion is involved in two such hydrogen bonds, acting as a proton donor in one of them and as a proton acceptor in the other. Each anion additionally provides its third O atom for the NH$\cdots$O hydrogen bonding to an adjacent pyrazine cation, leaving one terminal O atom. An infinite network of hydrogen bonds extends along the [x] direction (see Fig. 1c), but is limited to four neighbouring molecular subunits along the z direction (as it is interrupted by weak van der Waals contacts between adjacent pyrazinium cations). Comparison of the experimental and theoretical values of the $D{-}H$ and $H \cdots A$ bond lengths (D = donor, A = acceptor, see Table 2) shows that, as expected, the position of the H atom is poorly determined from X-ray methods.

3.2. β-polymorph with moderately strong NH$\cdots$O and OH$\cdots$N hydrogen bonds

The β-PHS cannot be obtained in a direct reaction between pyrazine and sulfuric acid, or *via* a phase transition from the α-form. It is accessed *via* slow decomposition of the reactive pyrazine complex of Ag^{II} (Leszczyński *et al.*, 2010). Similarly as for the α-form, there are four pyrazine cations and four hydrogen sulfate anions per unit cell of the β-form, but in the
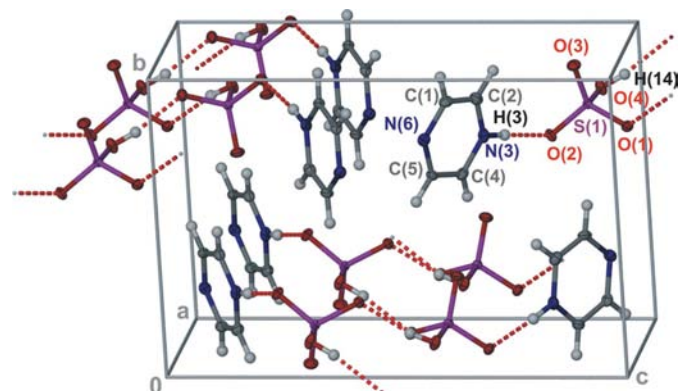
Figure 3
Unit cell of α-PHS at 103 (2) K. Hydrogen bonds have been indicated by dashed lines. The atomic ellipsoids are represented at the 50% probability level.
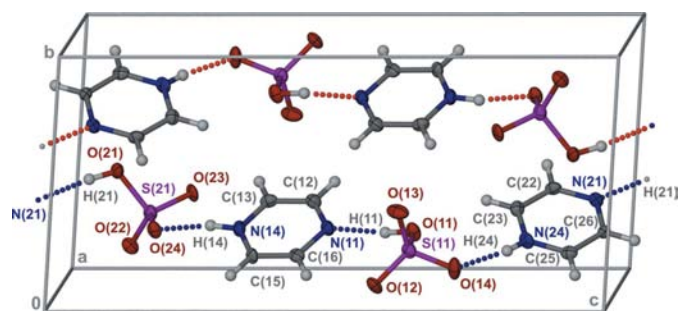
Figure 4
Unit cell of β-PHS. Hydrogen bonds have been indicated by dashed lines. The atomic ellipsoids are represented at the 50% probability level.

independent part of the unit cell there are now two cations and two anions (Fig. 4). However, both anions (as well as the cations) are structurally similar to each other as additionally confirmed by Hirshfeld surface analysis (Wolff *et al.*, 2005–2007) of intra-ionic distances (see Fig. S5 in SM).

The ions form alternating pseudohexagonal layers, with pyrazinium cations and the HSO_4^- anions deviating slightly from strict hexagonal symmetry (see Fig. S6). The layers are stacked in an ABCABC order, just like in the regular system. The ions self-assemble into infinite one-dimensional helical chains within each layer. The chains are composed of alternating cationic and anionic units interconnected by OH···N and NH···O hydrogen bonds. There are two such chains in the unit cell and both run along the z axis. The NH···O hydrogen bonds (also present in the structure of the α-polymorph) have been so far observed for pyrazinium nitrate, while no pyrazinium salt with OH···N interactions has been reported until now. Importantly, β-PHS is the only known pyrazinium salt where the pyrazinium cations act not only as donors but also as acceptors of hydrogen bonds.

The hydrogen bonds observed in β-PHS are close to linear and of moderate strength with NH···O bonds slightly shorter than OH···N ones (Table 2) and also shorter than their counterparts found for the α-polymorph. The graph sets (Etter *et al.*, 1990; Etter, 1990; Grell *et al.*, 1999) are $C_4^4(18)$ for the motif [–HOSO–HNCCN–HOSO–HNCCN–]$_n$ and $C_2^2(9)$ for the shortest link [–HOSO–HNCCN–]$_n$. The sequence of hydrogen bonds, namely the polar character of each individual chain, leads to the substantial local dipole moment. However, orientation of the chains is antiparallel with respect to each other, thus leading to null polarization of the crystal (Fig. 5).

A large volume of the α-form with respect to the β one ($\Delta V \simeq 5\%$) suggests that the former is the high-temperature phase of PHS. The solid-state DFT calculations indicate that the two phases have rather similar electronic energy, favouring the β-PHS over the α-form by 8 kJ mol^{-1} per formula unit of 17 atoms (the difference being within the error of the method).
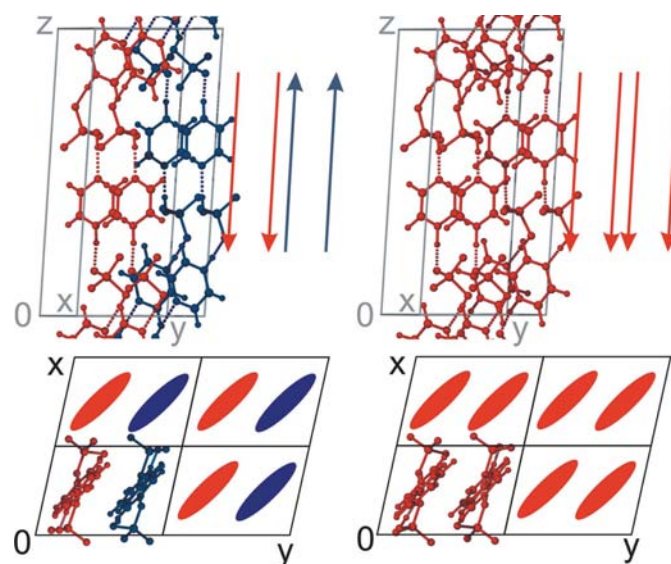
3.3. Hypothetical polar β′-form

As already pointed out, the polar character of the chains in β-PHS leads to a substantial local dipole moment which is cancelled out owing to the antiparallel orientation of the neighbouring chains. However, collective proton transfer along the hydrogen bonds in every second chain would result in a polar P1 phase. In this context, here we are interested in whether such a polar form of this polymorph could be stabilized.

To answer this question we have constructed the hypothetical P1 phase (β′) with mutual parallel orientation of the polar chains (Fig. 5) and calculated its energy relative to the energy of the experimental one ($P\bar{1}$). For this purpose, both the experimental $P\bar{1}$ and the hypothetical polar P1 unit cells of β-PHS were fully relaxed in the absence of an external electric field.

The DFT calculations showed that the two cells have very similar energies, the experimental $P\bar{1}$ phase being favoured by 2.5 kJ mol^{-1} (without vibrational corrections). Recalling the size of the system (17 atoms) and the error of the method (~ 5 kJ mol^{-1}), we can conclude that the two forms have in fact similar electronic energies. Thus, the β-form of PHS could indeed exhibit two distinct states of vastly different polarizations. Additionally, the structural changes between both polymorphic forms are also very small (*cf.* Table S2 and Fig. S7 in SM). Collective proton shifts within every second [–pyzH$^+$–HSO_4^-–] chain cause only a slight reorientation of the HSO_4^- units and a negligible ($< 0.5\%$) contraction of unit-cell parameters. Therefore, the *structural* component of the energy barrier for collective proton transfer within every second chain must be very small. It is however remarkable that the polar β-form is stable in the absence of an external electric field and it does not converge back to the $P\bar{1}$ form (although the low P1 symmetry in principle allows for that). This means that an energy barrier connected with hydrogen-bond breaking and formation arises between β- and β′-forms, and that the β′-form could indeed be a distinct entity even in the absence of an electric field.

This small energy difference between two polymorphs of opposite chain polarity might lead to a variety of phase transitions (producing all kinds of supercells based on a and b lattice vectors, including non-periodic modifications). However, the electrostatic inter-chain interaction (at an inter-chain distance of *ca* 5 Å) for PHS is certainly larger than for an interesting case of the hydrogen-bonded host–guest system with its inter-chain distance of *ca* 15 Å and large polar domains of > 100 Å (König *et al.*, 1997). This feature of PHS, we feel, diminishes the chance of the appearance of other polymorphic forms showing supercells.

Figure 5
Orientation of dipole moments generated by helical chains of hydrogen-bonded ions in the experimentally observed form of β-PHS (left) and a hypothetical polar β′-form of PHS (right).

Table 3
Comparison of the values of spontaneous polarization P for few important organic and inorganic FE materials (Horiuchi & Tokura, 2008; Andriyevsky & Doll, 2009; Rabe *et al.*, 2007; Kao, 2004).

RT = room temperature.

Material (organic)	P (C m^{-2})	Material (inorganic)	P (C m^{-2})
β-PHS (this work)	0.188; 0 K	PbTiO$_3$	0.50; 296 K
HdabcoReO$_4$	0.160; RT	BaTiO$_3$	0.26; RT
VDF	0.130; RT	SbSI	0.20; 270 K
TGS	0.038; 220 K	NaNO$_2$	0.10; 140 K
Thiourea	0.032; 120 K	LiNbO$_3$	0.07; RT
PST	0.025; 276 K	KH$_2$PO$_4$ (KDP)	0.048; 96 K

dabco = 1,4-diazabicyclo[2.2.2]octane; PHS = pyrazinium hydrogen sulfate; PST = potassium sodium tartrate tertahydrate; TGS = triglycine sulfate; VDF = vinylidene fluoride oligomer.

The dipole moment calculated for the ground state of the hypothetical polar β'-phase equals 1.7 D per unit; the dipole moment vector is lying nearly parallel to the z axis, as expected from the orientation of the chains and geometry of hydrogen bonds. The value of the corresponding calculated spontaneous polarization, 0.19 C m^{-2}, in the absence of an external electric field (Table 3), was found to be above the largest value of spontaneous polarizations reported so far for an organic compound (HdabcoReO$_4$, where dabco = 1,4-diazabicyclo[2.2.2]octane), also exceeding those usually observed for single-component polar organic molecules, hydrogen-bonded supramolecules or other organic–inorganic compounds. For example, well studied triglycine sulfate (TGS) exhibits polarization of 0.038 C m^{-2}, which is only 1/5 of that predicted for the hypothetical polar state of β-PHS. Additionally, the calculated polarization of β'-PHS is comparable to those of important inorganic ferroelectrics, being four times larger than that of the well known proton-transfer-type ferroelectric, KH$_2$PO$_4$ (KDP), and only 2.7 times smaller than that of the record-holding *inorganic* system, PbTiO$_3$ (Horiuchi & Tokura, 2008). Note that the method applied here for calculating dielectric polarization has proved to be very precise in the case of a similar organic–inorganic compound, *e.g.* TGS (Andriyevsky & Doll, 2009), with a theoretical value of 0.035 C m^{-2} and an experimental value of 0.038 C m^{-2}.

Since it has been observed for the titanate ceramics that the presence of a non-compensated dipole moment of the unit cell facilitates the large value of dielectric polarization in the presence of the external electric field, the large calculated polarization of β'-PHS is encouraging in the context of a possible ferroelectricity of this form, and it raises a question how the $P\bar{1} \rightarrow P1$ phase transition could be fulfilled in practice.

4. Conclusions

We report here the synthesis and crystal structures of two polymorphic forms of PHS, orthorhombic $P2_12_12_1$ (α) and triclinic $P\bar{1}$ (β), with hydrogen bonding unique among the known simple pyrazinium systems. The α-PHS is formed from infinite pyzH$^+$ and HSO$_4^-$ chains interconnected by OH$\cdots$O and NH$\cdots$O bonds extending in one dimension and limited to

four units (–pyzH$^+$–HSO$_4^-$–HSO$_4^-$–pyzH$^+$–) in another. The β-phase forms infinite chains of alternating pyzH$^+$ and HSO$_4^-$ ions interconnected by NH$\cdots$O and OH$\cdots$N bonds. The topologies of hydrogen bonds are new among the known pyrazinium salts.

Both polymorphs are stable at ambient conditions and exhibit no dipole moment. However, solid-state DFT calculations indicate that the hypothetical polar β'-form should exhibit substantial dielectric polarization of 0.19 C m^{-2} even in the absence of the external electric field, which is larger than for any other known organic material. The hypothetical polar β'-form is energetically equivalent to its related experimental β-form and the structural barrier expected for the proton transfer (β to β') is also very small. It should be of interest now to find whether the β to β' transition could be realised experimentally, for example by using a large external electric field or a laser impulse. Such a possibility would make the β-PHS a promising candidate for a new ferroelectric material.

References

Andriyevsky, B. & Doll, K. (2009). *J. Phys. Chem. Solids*, **70**, 84–91.
Barbour, L. J. (2001). *J. Supramol. Chem.* **1**, 189–191.
Blöchl, P. E. (1994). *Phys. Rev. B*, **50**, 17953–17979.
Clark, S. J., Segall, M. D., Pickard, C. J., Hasnip, P. J., Probert, M. J., Refson, K. & Payne, M. C. (2005). *Z. Kristallogr.* **220**, 567–570.
Etter, M. C. (1990). *Acc. Chem. Res.* **23**, 120–126.
Etter, M. C., MacDonald, J. C. & Bernstein, J. (1990). *Acta Cryst.* B**46**, 256–262.
Głowiak, T., Sobczyk, L. & Grech, E. (1975). *Chem. Phys. Lett.* **34**, 292–293.
Grell, J., Bernstein, J. & Tinhofer, G. (1999). *Acta Cryst.* B**55**, 1030–1043.
Horiuchi, S. & Tokura, Y. (2008). *Nature Mater.* **7**, 357–366.
Ilyukhin, A. B., Ma, G. & Glaser, J. (2000). Private communication. CCDC, Cambridge, England.
Kao, K.-C. (2004). *Dielectric Phenomena in Solids*, p. 247. New York: Academic Press.
Katrusiak, A. (1992). *J. Mol. Struct.* **269**, 329–354.
Katrusiak, A. (1993). *Phys. Rev. B*, **48**, 2992–3002.
Katrusiak, A. & Szafrański, M. (2006). *J. Am. Chem. Soc.* **128**, 15775–15785.
König, O., Bürgi, H.-B., Armbruster, T., Hulliger, J. & Weber, T. (1997). *J. Am. Chem. Soc.* **119**, 10632–10640.
Kresse, G. & Furthmüller, J. (1996*a*). *Comput. Mater. Sci.* **6**, 15–50.
Kresse, G. & Furthmüller, J. (1996*b*). *Phys. Rev. B*, **54**, 11169–11186.
Kresse, G. & Joubert, D. (1999). *Phys. Rev. B*, **59**, 1758–1775.
Leszczyński, P. J., Budzianowski, A., Derzsi, M., Dobrzycki, Ł., Cyrański, M. K. & Grochala, W. (2010). In preparation.
Oxford Diffraction (2002). *Xcalibur* User's Manual, Version 1.3. Oxford Diffraction, Wrocław, Poland.

Perdew, J. P., Burke, K. & Ernzerhof, M. (1996). *Phys. Rev. Lett.* **77**, 3865–3868.

Persistence of Vision (2004). *Raytracer*, Version 2.6. Persistence of Vision Pty Ltd, Williamstown, Victoria, Australia.

Pressprich, M. R., Willett, R. D., Paudler, W. W. & Gard, G. L. (1990). *Inorg. Chem.* **29**, 2872–2873.

Pressprich, M. R., Willett, R. D., Poshusta, R. D., Saunders, S. C., Harry, D. B. & Gard, G. L. (1988). *Inorg. Chem.* **27**, 260–264.

Rabe, K. M., Ahn, C. H. & Triscone, J.-M. (2007). Editors. *Physics of Ferroelectrics: A Modern Perspective Series: Topics in Applied Physics*, Vol. 105, p. 15. Berlin: Springer.

Sendil, K. & Ozgun, B. (2006). *Monatsh. Chem.* **137**, 1529–1533.

Sheldrick, G. M. (2008). *Acta Cryst.* A**64**, 112–122.

Wolff, S. K., Grimwood, D. J., McKinnon, J. J., Jayatilaka D. & Spackman, M. A. (2005–2007). *CrystalExplorer* 2.1(381), University of Western Australia, http://www.hirshfeldsurfacenet.blogspot.com/CrystalExplorer/.